with HCl; yields were between 96 and 99%.

Preparation of Manganocenes. Cp_2Mn (**1**) and $(MeCp)_2Mn$ (**2**) were synthesized similar to Wilkinson's procedures[2d,18] except that the sodium cyclopentadienides were prepared as mentioned above. For $(Me_5Cp)_2Mn$ (**9**) we followed Robbins et al.[5c]

Other Bis(mono- and disubstituted) Manganocenes. General Procedure. In a typical run 30 mmol of manganese(II) halide were suspended in 50 mL of THF. When $MnCl_2$ was used, $MnCl_2 \times 1.5$ THF[18] was formed in an exothermic reaction. The mixture was cooled to −20 °C, and 60 mmol of the dissolved cyclopentadienide were added with stirring and heated slowly to reflux. Within 6 h the solution became red. In some cases THF was replaced by higher boiling ethers like n-Bu_2O to make the reaction more efficient. After having removed the ether, the residue was extracted with 100 mL of pentane and washed with another four 20-mL portions of pentane. From the combined fractions the solvent was again removed, and the remainder was distilled at 8×10^{-2} Pa in an apparatus described in ref 20. Pure compounds were obtained when the distillation was kept slow (ca. 6 h) and when the film on the cooling finger was rejected twice at the beginning. Bis(ethyl-η^5-cyclopentadienyl)-manganese (**3**), bis(isopropyl-η^5-cyclopentadienyl)manganese (**4**), bis-(*tert*-butyl-η^5-cyclopentadienyl)manganese (**5**), bis(trimethylsilyl-η^5-cyclopentadienyl)manganese (**6**), and bis(1,2-dimethyl-η^5-cyclopentadienyl)manganese (**7**) were obtained in this way. Sublimation instead of distillation was used to isolate bis(tetramethyl-η^5-cyclopentadienyl)manganese (**8**) and bis(ethyltetramethyl-η^5-cyclopentadienyl)manganese (**10**). Preparative and analytical details are collected in Table VI.

NMR Measurements. When possible, the manganocene was freshly distilled into a 10-mm NMR tube equipped with a ground-glass joint; solvent and internal standard were added in case, and the sample was closed with a stopper. All spectra were recorded with a Bruker CXP 200 spectrometer with B VT 1000 temperature controller. Details such as instrumental parameters and temperature measurements were similar to those reported earlier.[34,45] Experimental shifts were measured relative to signals of the solvent or an internal standard and calculated relative to corresponding signals of isostructural ferrocenes to yield paramagnetic shifts, δ_T^{para} at a given temperature T with negative sign to low field. Details are given in the Supplementary Material. The errors were governed similarly by the line width Δ^{expt} and the above mentioned anisotropy effects: $\Delta^{expt} < 1$ kHz: δ better than ±0.5%; $\Delta^{expt} > 1$ kHz: δ ±1%. The temperature stability was better than ±0.3 K.

X-ray Structure Determination. A suitable single crystal was grown from a pentane solution at −78 °C after careful distillation of **6**. It was sealed under argon at dry ice temperature into a glass capillary and mounted on a four-circle diffractometer (Syntex $P2_1$). The monoclinic symmetry was checked by axial photographs and Delaunay reductions of the unit cell (TRACER). Exact cell dimensions were obtained by a least-squares fit of the parameters of the orientation matrix to the setting angles of 15 high angle reflections centered on the diffractometer. The crystal data as well as numerical details of the intensity data collection and structure refinement are given in Table III. One form of data was measured by a multispeed moving-crystal stationary-counter technique where the peak height at the calculated peak position served to determine the final scan speed. After Lp corrections a semiempirical absorption correction was applied because of the highly irregular crystal shape. This was based on scans at 10° intervals around the diffraction vectors of seven selected reflections near $\chi = 90°$ which served to determine the transmission curves (Syntex XTL). Since a reasonable density indicated $Z = 2$, the Mn atom was placed at the origin. (Due to the exceeding air and moisture sensitivity the experimental crystal density could not be determined). Subsequent Fourier and difference Fourier syntheses yielded the remainder of the molecule. After anisotropic refinement of the non-H atoms all hydrogens could be found in a difference synthesis. They were kept constant in further refinement cycles with the exception of those at the Cp ring which were refined isotropically. The function minimized in the refinement was $\Sigma w(|F_o| - |F_c|)^2$ with $w = k/\sigma^2(F_o)$ (SHELX 76). A final difference map was essentially featureless with the maxima in the vicinity of the methyl groups. Corrections for $\Delta f'$ and $\Delta f''$ were applied to all atoms. A detailed description of the data collection and refinement procedures is given elsewhere.[46] In this reference also the sources of the scattering factors are given.

Acknowledgment. We thank Professor P. Hofmann for helpful discussion. We are also grateful to the Fonds der Chemischen Industrie, Frankfurt for financial support.

Registry No. **1**, 73138-26-8; **2**, 32985-17-4; **3**, 101923-26-6; **4**, 85594-02-1; **5**, 101932-72-3; **6**, 101932-73-4; **7**, 101932-74-5; **8**, 101932-75-6; **9**, 67506-86-9; **10**, 101932-76-7.

Supplementary Material Available: Experimental NMR shifts, reference shifts of analogous ferrocenes, variable temperature NMR data for $(MeCp)_2Mn$, evaluation of $\Delta H°$ and $\Delta S°$, calculation of dipolar and contact shifts of the low-spin manganocenes, and additional crystal structure data tables of anisotropic temperature factors as well as observed and calculated structure factor amplitudes (11 pages). Ordering information is given on any current masthead page.

(36) Köhler, F. H. *J. Organomet. Chem.* **1976**, *110*, 235–246.
(37) Riemschneider, R.; Reichelt, E.; Grabitz, E. B. *Monatsh. Chem.* **1960**, *91*, 812–823.
(38) Köhler, F. H. *J. Organomet. Chem.* **1976**, *121*, C61–62.
(39) Riemschneider, R.; Reisch, A.; Horak, H. *Monatsh. Chem.* **1960**, *91*, 805–811.
(40) Davison, A.; Rakita, P. E. *Inorg. Chem.* **1970**, *9*, 289–294.
(41) Skattebøl, L. *J. Org. Chem.* **1964**, *29*, 2951–2956.
(42) Kohl, F. X.; Jutzi, P. *J. Organomet. Chem.* **1983**, *243*, 119–121.
(43) Feitler, D.; Whitesides, G. M. *Inorg. Chem.* **1976**, *15*, 466–468.
(44) King, R. B. *Metal Organic Syntheses*; Academic Press: New York, and London, 1965; Vol. I, pp 67–69.
(45) Köhler, F. H.; Hofmann, P.; Prössdorf, W. *J. Am. Chem. Soc.* **1981**, *103*, 6359–6367.
(46) Schmidbaur, H.; Herr, R.; Müller, G.; Riede, J. *Organomet.* **1985**, *4*, 1208–1213.

Fourier-Transform Infrared Linear Dichroism: Stretched Polyethylene as a Solvent in IR Spectroscopy

Juliusz G. Radziszewski and Josef Michl*

Contribution from the Department of Chemistry, University of Utah, Salt Lake City, Utah 84112. *Received October 18, 1985*

Abstract: The infrared linear dichroism of several dozen symmetrical organic molecules of low polarity has been measured on their solid solutions in stretched polyethylene and stretched perdeuterated polyethylene. Both saturated and unsaturated molecules, ranging in size from triatomics to tetracyclic aromatics, have been used. The orientation factors are dictated primarily by molecular shape, making these simple measurements useful for the determination of absolute polarizations of infrared as well as UV–visible transitions. The potential usefulness of the method for studies of molecular geometry and conformation is emphasized and illustrated on the simple case of aniline.

Among the characteristics of a transition in optical spectroscopy, the most fundamental ones are the energy (light frequency), intensity, and polarization, i.e., transition moment direction in the molecular framework. Whereas the first two have seen much use

0002-7863/86/1508-3289$01.50/0

Table I. Orientation Factors at Room Temperature[a]

	compound	K_z	K_y	K_x
1	*p*-terphenyl	0.78	0.12	0.10
2	2,3-dimethylanthracene	0.70	0.17	0.12
3	diphenylacetylene	0.64	0.22	0.22
4	perylene	0.63	0.23	0.15
5	anthracene[b]	0.62	0.26	0.11
6	4,4′-dibromobiphenyl[c]	0.61	0.23	0.17
7	1,6:8,13-ethanediylidene[14]annulene	0.61	0.24	0.15
8	4,4′-dibromobiphenyl-d_8[c]	0.60	0.24	0.18
9	acridine[b]	0.60	0.25	0.13
10	2-methylpyrene	0.60	0.32	0.06
11	*syn*-1,6:8,13-bis(methano[14]annulene)	0.59	0.25	0.16
12	fluoranthene	0.58	0.31	0.11
13	2,3-dibromonaphthalene	0.57	0.29	0.15
14	phenanthrene	0.56	0.33	0.11
15	phenazine[b]	0.55	0.24	0.21
16	2,3-dimethylnaphthalene	0.55	0.30	0.14
17	*p*-diiodobenzene	0.53	0.31	0.17
18	*p*-xylene	0.52	0.26	0.22
19	*p*-dimethoxybenzene	0.52	0.28	0.19
20	9-methylanthracene	0.52	0.29	0.19
21	*p*-dibromobenzene	0.52	0.30	0.18
22	pyrene[d]	0.52	0.34	0.12
23	fluorene	0.51	0.34	0.12
24	*N*-methylcarbazole	0.51	0.31	0.18
25	biphenyl[c]	0.50	0.31	0.20
26	biphenyl-d_{10}[c]	0.50	0.31	0.20
27	6,7-dihydroacenaphtho[5,6-*cd*][1,2,6] thiadiazine	0.50	0.36	0.14
28	1,2-dibromoacenaphthylene	0.49	0.32	0.20
29	dibenzothiophene	0.49	0.32	0.17
30	acenaphtho[5,6-*cd*][1,2,6]thiadiazine	0.49	0.36	0.13
31	1,2,4,5-tetrachlorobenzene	0.48	0.31	0.20
32	naphthalene	0.47	0.33	0.18
33	9,10-dimethylantracene	0.47	0.34	0.18
34	2,3-dimethylquinoxaline	0.46	0.33	0.21
35	durene	0.45	0.32	0.22
36	1,2-diphenylacenaphthylene	0.44	0.35	0.21
37	*p*-dibromotetrafluorobenzene	0.43	0.36	0.22
38	nitrobenzene	0.43	0.34	0.24
39	acenaphthylene	0.42	0.38	0.20
40	quinoxaline	0.42	0.30	0.28
41	acenaphthene	0.41	0.38	0.21
42	triphenylene	0.41	0.41	0.17
43	perchlorocyclopentadiene	0.40	0.33	0.26
44	*o*-dibromobenzene	0.38	0.37	0.26
45	*o*-diiodobenzene	0.38	0.36	0.27
46	*m*-dibromobenzene	0.37	0.36	0.28
47	*m*-diiodobenzene	0.37	0.36	0.26
48	rhodium(II) acetate	0.37	0.37	0.27
49	benzene	0.37	0.37	0.24
50	benzene-d_6	0.36	0.36	0.26
51	dodecamethylcyclohexasilane	0.36	0.36	0.27
52	*o*-xylene	0.36	0.35	0.27
53	chloroform	0.358	0.358	0.283
54	bromoform	0.353	0.350	0.293
55	iodoform	0.350	0.350	0.300
56	carbon tetrachloride	0.33	0.33	0.33

[a] In linear low-density polyethylene. [b] From ref 18. [c] From ref 27. [d] From ref 14.

Table II. Orientation Factors and Vibrational Frequencies and Symmetries for Triatomic Molecules[a]

compd	$\bar{\nu}$ (cm^{-1})	K(PE)	K(PE-d_4)	assignment
OCS	516	0.25 (*x*,*y*)		ν_2 fundamental
	856	0.54 (*z*)	0.40 (*z*)	ν_1 fundamental
	1038	0.50 (*z*)	0.40 (*z*)	2 × 516 = 1032
	1706	0.50 (*z*)	0.40 (*z*)	2 × 856 = 1712
	1881	0.50 (*z*)	0.39 (*z*)	2 × 516 + 856 = 1888
	1983	0.50 (*z*)	0.40 (*z*)	ν_3 fundamental O=^{13}C=S
	2041	0.50 (*z*)		ν_3 fundamental
	2894		0.40 (*z*)	2041 + 856 = 2897
	3065	0.48 (*z*)	0.40 (*z*)	2 × 516 + 2041 = 3073
	4059	0.49 (*z*)	0.40 (*z*)	2 × 2041 = 4082
CO_2	660	0.29 (*x*,*y*)	0.28 (*x*,*y*)	ν_2 fundamental
	2332	0.40 (*z*)	0.36 (*z*)	ν_3 fundamental
N_2O	585	0.30 (*x*,*y*)	0.29 (*x*,*y*)	ν_2 fundamental
	1280	0.41 (*z*)	0.37 (*z*)	ν_1 fundamental
	2215	0.42 (*z*)		ν_3 fundamental
	2552	0.41 (*z*)		2 × 1280 = 2560
	3466	0.41 (*z*)		1280 + 2215 = 3495

[a] Low-temperature orientation factors K in linear low-density polyethylene (PE) and high-density perdeuterated polyethylene (PE-d_4).

Table III. Orientation Factors (77 K)[a]

	compound	K_z	K_y	K_x
6	4,4′-dibromobiphenyl[b]	0.66	0.24	0.10
8	4,4′-dibromobiphenyl-d_8[b]	0.64	0.23	0.12
12	fluoranthene	0.61	0.32	0.07
14	phenanthrene	0.56	0.34	0.10
22	pyrene[c]	0.56	0.33	0.10
26	biphenyl-d_{10}[b]	0.56	0.31	0.14
25	biphenyl[b]	0.54	0.28	0.16
57	carbonyl sulfide	0.51	0.25	0.25
58	carbon disulfide	0.49	0.25	0.25
59	nitrous oxide	0.42	0.30	0.30
60	dimethyl ether	0.42	0.31	0.28
61	ethylene	0.40	0.38	0.22
62	dimethylacetylene	0.40	0.30	0.30
63	carbon dioxide	0.39	0.29	0.29
49	benzene	0.38	0.38	0.24
53	chloroform	0.38	0.38	0.25
64	isobutene	0.38	0.36	0.26
65	methylacetylene	0.38	0.31	0.31
54	bromoform	0.37	0.37	0.26
66	chloroform-*d*	0.37	0.37	0.26
50	benzene-d_6	0.36	0.36	0.26

[a] Linear low-density polyethylene. [b] From ref 27. [c] From ref 14.

in structural chemistry, transition polarizations have been exploited a good deal less. This limited use is probably due to a combination of factors, the most important being the notion that polarization measurements are difficult to perform and more difficult to interpret, which seems to prevail among those most likely to benefit from their use.[1]

While this might have been a correct perception at one time, both for UV–visible spectroscopy and infrared spectroscopy, developments in the use of anisotropic solvents in the last two decades have certainly changed the situation for UV–visible spectroscopy. Both the use of stretched polymers and the use of liquid crystals as solvents produce quite predictable partial alignment of solute molecules, so that the determination of absolute polarization directions in the UV–visible region is now easy. Several hundred examples are quoted in ref 2–5.

In spite of several encouraging applications of polarized UV–visible measurements in stretched polymers to conformational problems, e.g., in the steroid series,[6] it is clear that the potential of UV–visible spectroscopy for structural work is limited: many interesting structures have no characteristic UV–visible absorption

(1) See, for instance, the discussion on p 162 of the following textbook: Harris, D. C.; Bertolucci, M. D. *Symmetry and Spectroscopy*; Oxford University Press: New York, 1977.

(2) Nordén, B. *Appl. Spectrosc. Rev.* **1978**, *14*, 157. Johansson, L. B.-A.; Lindblom, G. *Q. Rev. Biophys.* **1980**, *13*, 63.

(3) Thulstrup, E. W. *Aspects of the Linear and Magnetic Circular Dichroism of Planar Organic Molecules*; Springer-Verlag: New York, 1980. Michl, J.; Thulstrup, E. W. *Spectroscopy with Polarized Light. Solute Alignment by Photoselection, in Liquid Crystals, Polymers, and Membranes*; VCH Publishers, Inc.: Deerfield Beach, FL, 1986.

(4) Thulstrup, E. W.; Michl, J. *J. Phys. Chem.* **1980**, *84*, 82.

(5) Thulstrup, E. W.; Michl, J. *J. Am. Chem. Soc.* **1982**, *104*, 5594. The abbreviation TEM refers both to the trial-and-error method for separation of overlapping peaks of different polarization and to the initials of the authors who proposed the model; ref 20 and the following: Michl, J.; Thulstrup, E. W.; Eggers, J. H. *J. Phys. Chem.* **1970**, *74*, 3878. Unlike competing models, the TEM model uses two independent second moments for the orientation distribution function (K_y, K_z); see ref 3 and 4.

(6) Yogev, A.; Sagiv, J.; Mazur, Y. *J. Chem. Soc., Chem. Commun.* **1973**, *943*. Yogev, A.; Riboid, J.; Marero, J.; Mazur, Y. *J. Am. Chem. Soc.* **1969**, *4559*.

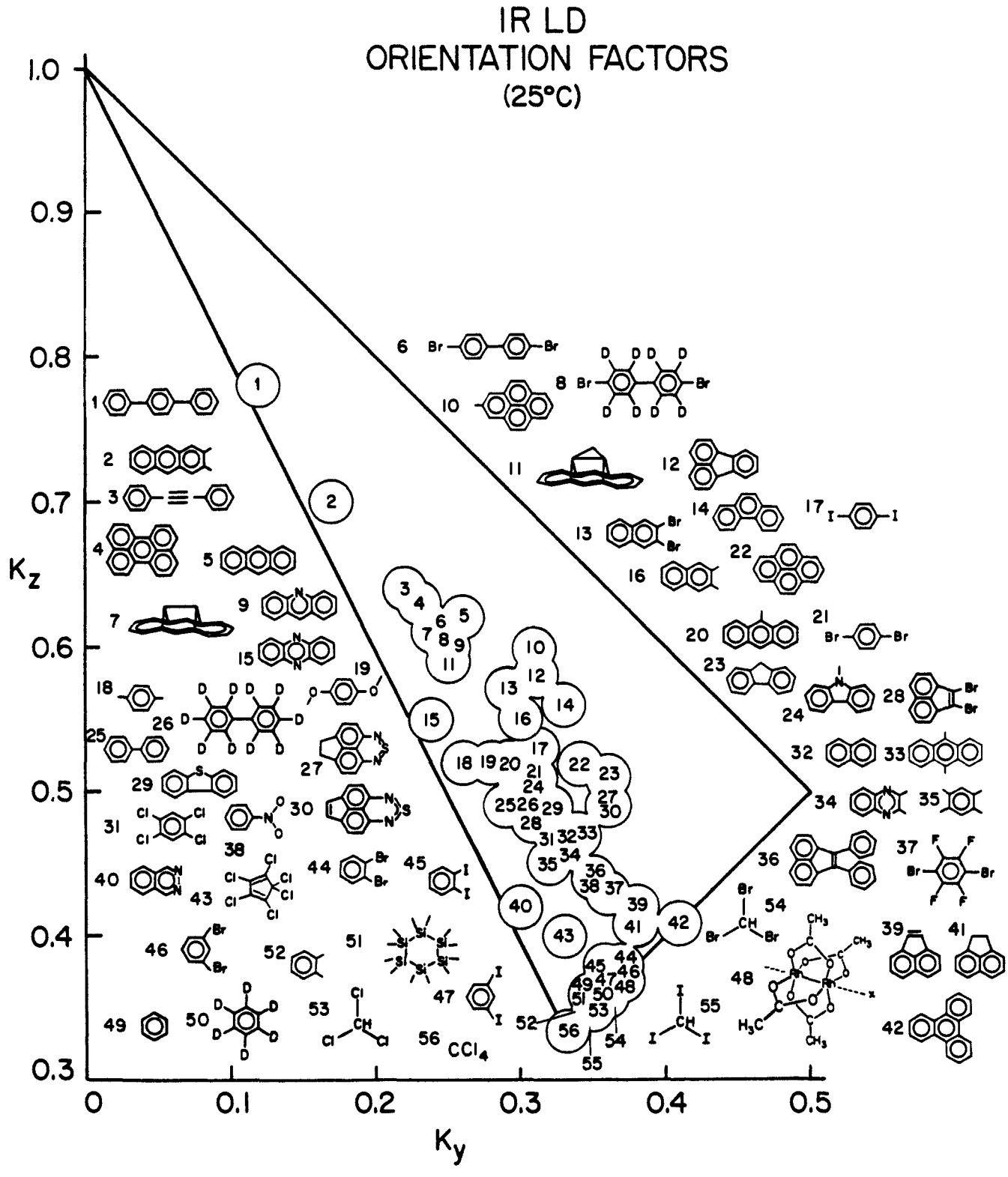

Figure 1. Orientation factors in stretched linear low-density polyethylene at room temperature.

in the accessible region, and the bands exhibited by those which do are often broad and have a tendency to overlap if more than one chromophore is present. Clearly, infrared spectroscopy, with its generally larger number of quite narrow bands for very many of the interesting structures, and particularly with its far more impressive record in structure elucidation in the hands of the organic chemist,[7] is the candidate of choice for further developments in the application of polarization measurements to structural chemistry.

In view of its extreme experimental simplicity, the use of stretched polymers as anisotropic solvents appears as a very attractive choice. Early attempts to measure polarizations of IR bands of solutes in stretched polymers using dispersive instruments ran into difficulties because of the much lower absorption intensities in the IR relative to UV–visible region, and usually only a few most intense bands were observed (e.g., ref 8–13). However,

(7) Bellamy, L. J. "The Infrared Spectra of Complex Molecules"; John Wiley and Sons: New York, 1975; Vol. 1 and 2.

(8) Kern, J. *Z. Naturforsch. A* **1962**, *17*, 271.
(9) Jakobi, H.; Novak, A.; Kuhn, H. *Z. Electrochem.* **1962**, *66*, 863.
(10) Gagakhedkar, N. S.; Namjoshi, A. V.; Tamhane, P. S.; Chaudhuri, N. K. *J. Chem. Phys.* **1974**, *60*, 2584.

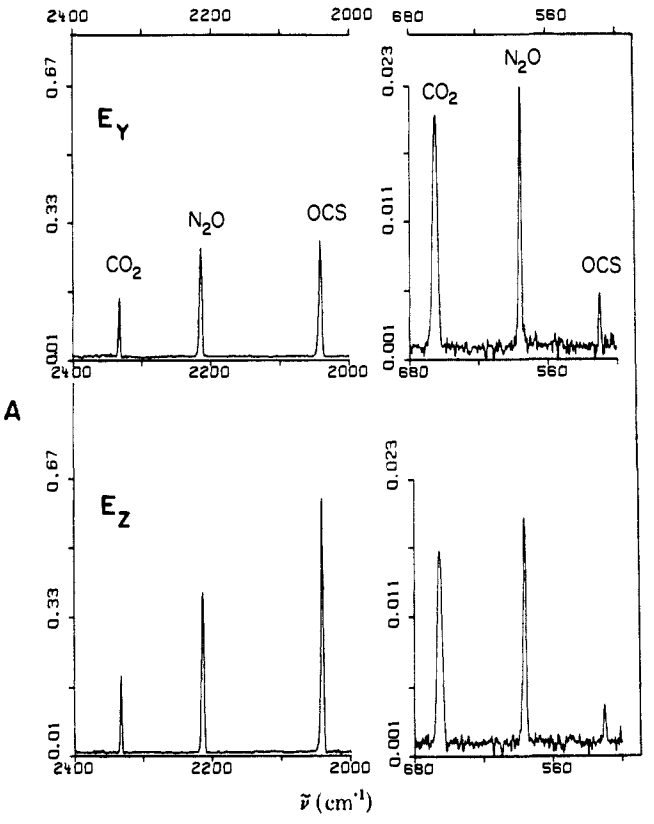

Figure 2. Polarized Fourier-transform IR spectra of CO_2, N_2O, and OCS in stretched linear low-density polyethylene. In E_Z (E_Y), the electric vector of the light is oriented parallel (perpendicular) to the stretching direction Z. See also Table II and text.

the use of modern instrumentation and of thicker sheets of polyethylene easily permits accurate IR polarization measurements.[14-18] This has changed the situation dramatically, and the way now appears to be clear for an exploitation of polarized IR measurements in structural chemistry.

It has already been noted[14,16] that the combined use of polyethylene and perdeuterated polyethylene permits the coverage of the whole IR region from far-IR to near-IR. In the present paper, we show that (i) the stretched sheet method is applicable to a wide variety of structural types and molecular sizes, from triatomics to multiring structures and from saturated molecules to olefins and aromatics; (ii) the partial orientation of solutes of all of the above kinds in stretched polyethylene is dictated primarily by their shape, as already demonstrated previously by UV–visible[5] and fluorescence[19] spectroscopy for aromatics; and (iii) the stretched sheet method is applicable to structural problems, e.g., it readily demonstrates the nonplanarity of aniline as contrasted with the planarity of nitrobenzene. All of the molecules under study except aniline had at least C_{2v} or D_2 symmetry, which dictated the three possible directions for transition moments.

Experimental Section

Materials. (a) Chemicals. Most of the solutes were obtained from commercial sources and were purified by gradient sublimation, crystallization, or distillation as necessary.

Table IV. Vibrations of Nitrobenzene and Their Symmetries

	$\tilde{\nu}$ (cm^{-1})				
symmetry	lit.[a]	PE	K(PE)	K(PE-d_4)	assignment[a]
A_1	399				
	680	682	0.45		
	851	851	0.44		NO_2 s def.
	1002	1003	0.44		
	1021	1022	0.44		
	1108	1110	0.43		CN stretch
	1176	1174	0.46		
		1245	0.45		
	1348	1347	0.45		NO_2 s stretch
		1405	0.45		
	1480	1481		0.43	
	1588	1590	0.44		
		1721	0.45		
		1802	0.44		
		1901	0.44		
		1977	0.45		
	3050	3048		0.43	
	3080	3078		0.43	
	3080	3084		0.42	
B_1	180				
	425				
	675	676	0.22		ring def. o.p.
	704	702	0.23		NO_2 wag
	791	791	0.23		CH bend o.p.
	936	931	0.23		
	998				
B_2	265				
	531				
	613				
	1069	1068	0.31		
		1093	0.31		
	1162	1160	0.33		
	1308	1307	0.31		
	1316	1316	0.31		
	1460	1461		0.33	
		1501	0.32		
	1525	1534	0.33		NO_2 as stretch
	1612	1608/1621	0.32		
		1762	0.32		
		1957	0.31		
	3080	3080	0.31		
	3080	3087	0.31		

[a] Reference 28.

Linear low-density polyethylene (LDPE) pellets were obtained from Dow Chemical Co. and high-density perdeuterated polyethylene (HDPE-d) chips (98% d) from Merck Co., Inc.

(b) Polymer Sheets. Polyethylene sheets 0.05 to 2.00 mm thick were prepared by melting pellets of linear LDPE in a hot press at 150–165 °C, pressing them (~2000 psi), and either quenching the resulting sheets in ice water or annealing them in a press at 90 °C overnight. Rectangular pieces of the polymer sheet (~15 × 30 mm, with long sides cut slightly concave for more uniform stretching) were stretched 450% at room temperature either in a home-built stretcher or on an Instron stretcher. They were kept under tension for about 30 min before use. Stretching ratios up to 600% were tested and yielded nearly identical results. Perdeuterated HDPE-d requires a lower press temperature (140–155 °C) and cannot be annealed in air for longer times. Since it contains much less amorphous phase it is more difficult to stretch. Still, it can be stretched up to 400% at ~40 °C.

The surfaces of the samples were subsequently scratched with tissue paper in order to suppress interference fringes. Reference spectra of both polarized base lines were obtained on the blank stretched sample before the solute was introduced.

Sample Preparation. Depending on the volatility of the solutes various methods of imbedding them in polyethylene were used.

(a) Involatile Solutes. Solids of low vapor pressure were introduced to the polyethylene matrix from a solution in spectral quality chloroform, deuterated chloroform, benzene, or cyclohexane. Usually, the stretched polyethylene sheet was soaked in the solution for a period ranging from a few minutes to a few days either at room temperature or above, up to 60 °C maximum. Relaxation of the stretched polyethylene at this temperature is not measurable even after 2 days of soaking, but our samples of polyethylene lose their uniaxial orientation in about 10 min at 90 °C. Before spectral measurement, the solvent was removed on a vacuum line

(11) Ingwall, R. T.; Gilon, C.; Goodman, M. *J. Am. Chem. Soc.* **1975**, *97*, 4356.
(12) Jonáš, I.; Nordén, B. *Spectrochim. Acta, Part A* **1976**, *32*, 427.
(13) Bauer, G. *Monatsh. Chem.* **1971**, *102*, 1797.
(14) Radziszewski, J. G.; Michl, J. *J. Phys. Chem.* **1981**, *85*, 2934.
(15) Konwerska-Hrabowska, J.; Chantry, G. W.; Nicol, E. A. *Int. J. Infrared Millimeter Waves* **1981**, *2*, 1135.
(16) Ovaska, M.; Kivinen, A. *J. Mol. Struct.* **1983**, *101*, 255.
(17) Other linear polymers can also be used: Kivinen, A.; Ovaska, M. *J. Phys. Chem.* **1983**, *87*, 3809.
(18) Radziszewski, J. G.; Michl, J. *J. Chem. Phys.* **1985**, *82*, 3527.
(19) Hennecke, M.; Fuhrmann, J. *Colloid Polym. Sci.* **1980**, *258*, 219. Fuhrmann, J.; Hennecke, M. *Makromol. Chem.* **1980**, *181*, 1685.

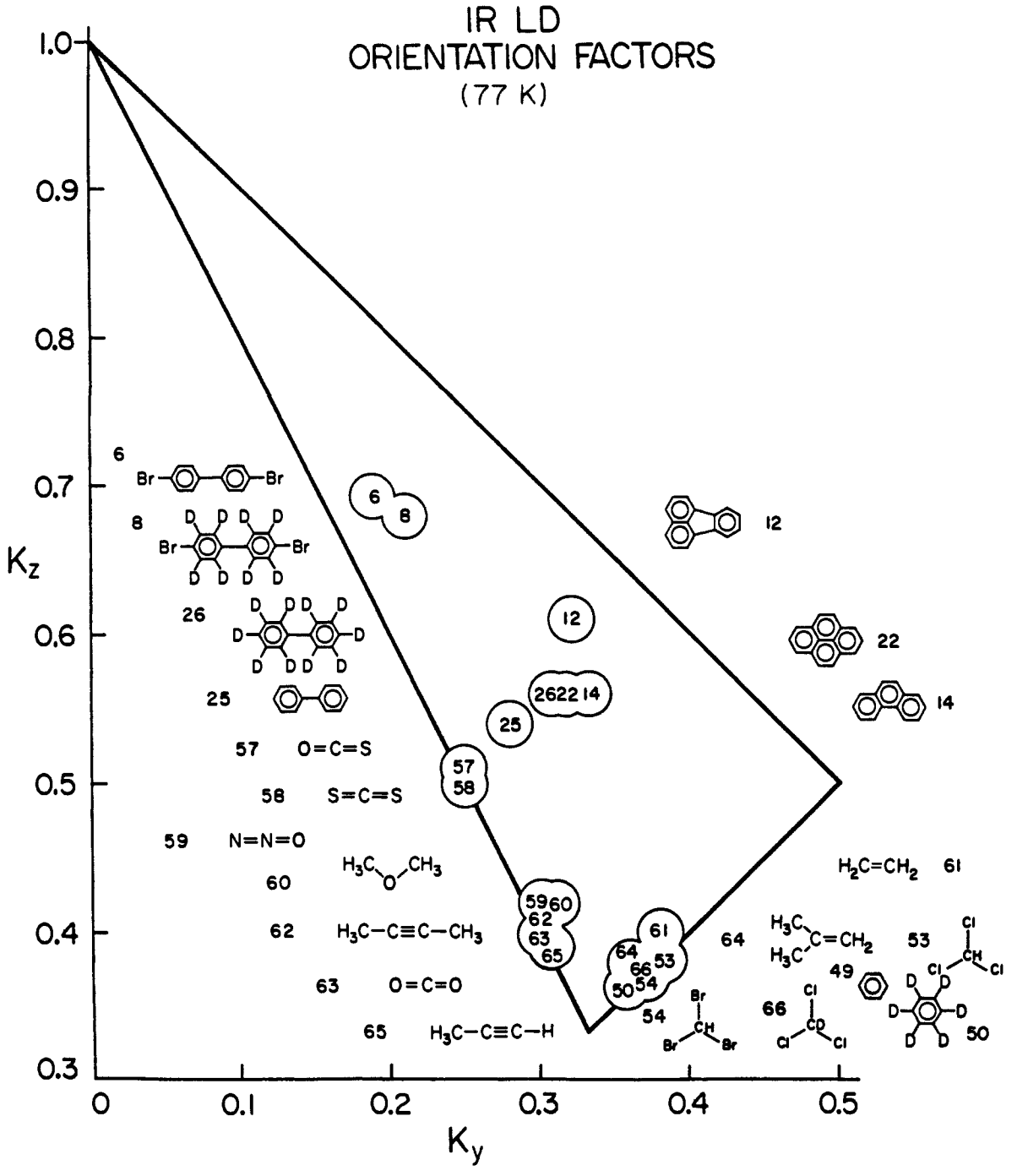

Figure 3. Orientation factors in stretched linear low-density polyethylene at 77 K.

(0.5–2 h at 10^{-4} Torr, depending on sample thickness).

It is also possible to first saturate an unstretched polyethylene sample with the solute, then stretch the sample, and after the spectral measurements are complete to remove the solute by washing with excess solvent. This procedure consumes much more time and requires larger amounts of the compound to start with but yields very similar results.

(b) Poorly Soluble Involatile Solutes. In special cases, when the concentration of the solute introduced into polyethylene by the above procedure was insufficient even after soaking at 60 °C, or when its solubility in all the above solvents was poor, another method was used. Polyethylene pellets were dissolved in *p*-xylene at 50 °C, the solute was added, and the solution was vigorously stirred until it became very viscous. Then it was deposited on a microscope slide, cooled to room temperature, and dried in air for many hours. Residual *p*-xylene was removed on a vacuum line. Only relatively small samples (1 × 3 × 3 mm) could be prepared by using this method because of microcavities left by bubbles of evaporating *p*-xylene. This problem can be solved by making much thinner films (0.05 mm) and by using ten or twenty sheets for the spectral measurement. Reference samples were prepared in the same way, using polyethylene only. The base line could be reproduced to a satisfactory degree. In the case of very heat resistant compounds the xylene-free solid solution was cut into small pieces and pressed in a hot press under N_2 atmosphere to form a film. If the dopant concentration was kept below about 2% no IR bands due to microcrystals were observed.

In all the above cases the surfaces of the final sample were washed with methanol in order to remove crystallites.

(c) Volatile Solutes. Highly volatile solutes were introduced into polyethylene from the vapor phase by storing a polymer sheet over a small amount of liquid or crystals of the solute in an evacuated vial for a few days. These samples require rapid handling and measurement or the use of lower temperatures in order to avoid solute loss by evaporation.

(d) Gaseous Solutes. For gaseous solutes low temperatures were employed, using a closed cycle helium cryostat (Air Products Co.). Stretched samples of both perdeuterated and normal polyethylene were pressed to a CsI window attached to the cold end, using a mask with two $^3/_8$ in. openings for each sample. The shroud was then evacuated and the gaseous solute released into it, typically at 600–650 torr. Depending on the desired optical density, polyethylene samples were kept in the gas atmosphere for a period ranging from a few minutes to a few hours. The sample was cooled to ~20 K and then slowly warmed up to a tempera-

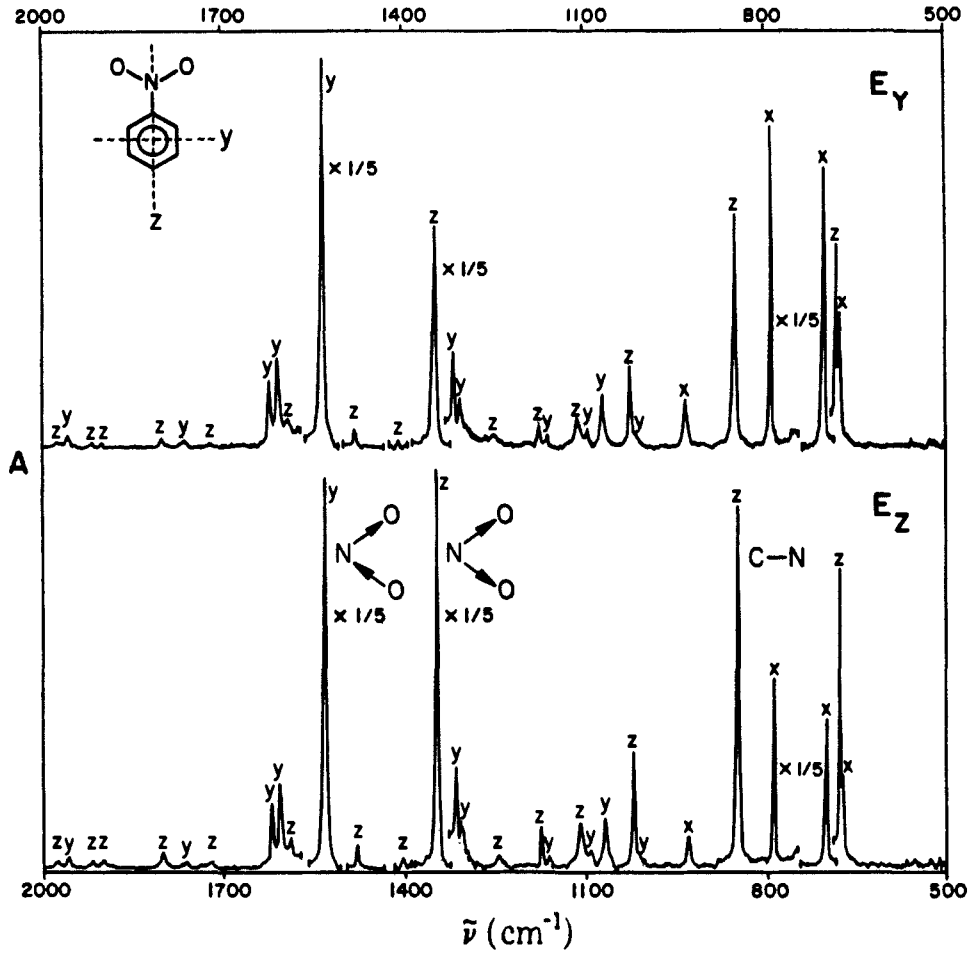

Figure 4. Polarized Fourier-transform IR spectra of nitrobenzene in stretched polyethylene. Parts of the spectrum (715–735 and 1415–1500 cm^{-1}) blocked by linear low-density polyethylene were obtained by using polyethylene-d_4. In E_Z (E_Y), the electric vector of the light is oriented parallel (perpendicular) to the stretching direction Z. See also Table IV and text.

ture about 10 deg higher than the melting point of the compound, while pumping on the cryostat, in order to remove the solid condensed on surfaces. At such temperatures, the rate of diffusion to the surface from inside the polyethylene sheet is negligible. After cooling back to 10 K (or 77 K), both polarized spectra for each sample were measured. Subsequently, the samples were warmed up, with the vacuum line attached to the cryostat, and kept at room temperature. After complete gas removal they were cooled to 10 K (or 77 K) and polarized base lines were measured. In some cases spectra of several gases were measured simultaneously on a mixture.

Spectral Measurements. Infrared spectra were recorded on Nicolet 6000 (4000–400 cm^{-1}) and Nicolet 8000-HV (4000–50 cm^{-1}) spectrometers with a resolution of 1 cm^{-1}, using aluminum grid polarizers, IPG-225 for the mid-IR region, and IPG-223 for the far-IR region (Cambridge Physical Sciences, Ltd.). For room temperature measurements, the polymer sheets were kept in a home-made holder. In all low-temperature measurements a closed-cycle helium refrigerator as described above was used for gaseous samples.

The principal sources of error in the determination of the orientation factors are base line uncertainty and limited reproducibility for weak peaks, solute evaporation in the case of very volatile samples, and imperfections in the optical setup. The factors which contribute to the latter are incomplete light polarization by the polarizers, light depolarization by the sample and the optical elements, imperfect polarizer and sample alignment, and nonuniformities in the stretched polymer. All of these tend to cause a mixing of the ideally polarized spectra, such that the actually recorded spectra are not $E_Z(\tilde{\nu})$ and $E_Y(\tilde{\nu})$ but rather are approximately given by $E_Z(\tilde{\nu})\cos^2\alpha + E_Y(\tilde{\nu})\sin^2\alpha$ and $E_Z(\tilde{\nu})\sin^2\alpha + E_Y(\tilde{\nu})\cos^2\alpha$, where α is a small angle characteristic of the optical imperfections. While the orientation factors[3-5,20] K_x, K_y, and K_z derived from the ideal polarized spectra $E_Z(\tilde{\nu})$ and $E_Y(\tilde{\nu})$ by the procedures described in the text add up to unity, $\sum_u K_u = 1$, the orientation factors actually obtained often add up to a little less. Straightforward algebra shows that in the absence of other errors the observed sum is given by

$$\sum_u K_u(\text{obsd}) = 1 - \tan^2\alpha \sum_u \frac{K_u - \frac{1}{3}}{\tan^2\alpha + \frac{2}{3}(1 - \tan^2\alpha)/(1 + K_u)}$$

The actually observed sums range from 0.98 to 1.01, suggesting that the errors in the individual K_u values measured in our experiments do not exceed ±2%. With special effort and averaging of several measurements, the accuracy is improved to about ±1%, but this was not considered necessary for the present purposes.

Results and Discussion

Molecular Orientation. The polarization ratio d_f for each observed transition f (f = 1, 2, ...) was obtained as the ratio of its integrated peak area in the spectrum $E_Z(\tilde{\nu})$, measured with the electric vector of the light parallel to the sheet stretching direction Z, to that in the spectrum $E_Y(\tilde{\nu})$, measured with the electric vector perpendicular to Z:

$$d_f = \int_f E_Z(\tilde{\nu})\,d\tilde{\nu} \Big/ \int_f E_Y(\tilde{\nu})\,d\tilde{\nu} \qquad (1)$$

In a few instances of overlapping peaks, the stepwise reduction procedure was used to determine d_f in the manner usual in UV–visible spectroscopy.[3,5,20]

The dichroic ratios (or stepwise reduction factors) d_f were converted into the orientation factors K_f by using the standard assumptions of the TEM model:[5] all solvent effects are isotropic, the sample is uniaxial, and intrinsically purely polarized spectral features are recognizable in the spectra even if they mutually overlap. These assumptions yield

$$K_f = \langle\cos^2\phi_f^Z\rangle = d_f/(2 + d_f) \qquad (2)$$

$$\sum_{u=x,y,z} K_u = 1 \qquad (3)$$

(20) Thulstrup, E. W.; Michl, J.; Eggers, J. H. *J. Phys. Chem.* **1970**, *74*, 3868.

Table V. Vibrations of Aniline and Their Symmetries

symmetry	$\bar{\nu}$ (cm^{-1}) CCl_4[a]	$\bar{\nu}$ (cm^{-1}) PE	K^{LT}(PE)	K^{RT}(PE)	polarization	assignment[a]
A′	501	503	0.18	0.20	*x*	X-sens o.p.
	689	690	0.18	0.20	*x*	ring def o.p.
	747	754	0.18	0.20	*x*	CH bend o.p.
	823	824	0.49		*z*	
	874	873	0.18		*x*	CH bend o.p.
	996	996	0.46	0.42	19° (17°)[b]	
	1028	1028	0.46	0.42	19° (17°)[b]	
	1173	1174	0.50	0.44	*z*	
	1190	1193	0.50		*z*	
		1266	0.49		*z*	
	1278	1279	0.49	0.44	*z*	CN stretch
	1501	1501	0.49	0.44	*z*	
	1527	1525	0.50		*z*	
	1560	1557	0.50		*z*	
	1603	1602	0.46	0.42	20° (17°)[b]	NH_2 scissoring
	1618	1617	0.50	0.44	*z*	ring stretch
		1712	0.49		*z*	
	1768	1763	0.49		*z*	
	1825	1821	0.50		*z*	
	1838	1837	0.50		*z*	
	1933	1930	0.51		*z*	
	3074	3072	0.50		*z*	CH stretch
A′	3401	3393	0.47	0.41	17° (21°)[b]	NH_2 s stretch
A″	808	814	0.32		*y*	
	957	950	0.33		*y*	
	968	966	0.32		*y*	
	1054	1053	0.33		*y*	
	1115	1114	0.33		*y*	
	1152	1153	0.33		*y*	
	1308	1309	0.33		*y*	CH bend i.p.
	1324	1325	0.33	0.36	*y*	ring stretch
	1340	1339	0.32		*y*	
	1590	1590	0.32	0.36	*y*	ring stretch
	1690	1688	0.33		*y*	
	1918	1913	0.32		*y*	
	3040	3034	0.33		*y*	CH stretch
	3094	3094	0.33		*y*	CH stretch
	3485	3479	0.32	0.36	*y*	NH_2 as stretch

[a] Reference 29. [b] Angle between the transition moment and the *z* axis as obtained from low-temperature dichroism. The values in parentheses were obtained from room temperature dichroism.

Here, K_f is the average value of the square of the cosine of the angle ϕ_f^Z between the fth transition moment and the stretching direction Z.

The observed magnitude of K_f for any of the IR transitions of a solute attained only one of at most three distinct values within the limits of experimental accuracy (Table I). This corresponds well to the expectation that each transition moment is directed along one of the three symmetry-adapted axes, *x*, *y*, or *z*, in the high-symmetry molecules used in the measurements. Thus, the up to three distinct K_f values correspond to K_x, K_y, and K_z and provide information about the average alignment of the symmetry-adapted molecular axes with the stretching direction Z. Only two distinct K_f values were observed for those molecules whose symmetry is such that two of the symmetry-adapted axes transform according to a doubly degenerate irreducible representation (e.g., *x* and *y* in the C_{3v} group, $K_x = K_y$). As mentioned in the Experimental Section, the sum of the three K_u values equaled unity within the experimental error of 1 or 2%.

The labeling of the molecular axes is determined by the convention[3,5] $K_x \leq K_y \leq K_z$. The identification of the *x*, *y*, and *z* labels with the individual symmetry axes in a molecule represents an absolute polarization assignment. It was automatic if two of the K_u's coincided by symmetry, cf. eq 3. For instance in $CHCl_3$, only two distinct orientation factors are observed, as expected from the C_{3v} molecular symmetry. Since $K_z \geq K_y \geq K_x$ by definition, *z*-polarized transitions show a positive dichroism and *x*-polarized ones a negative dichroism in the absence of overlap. The question is only, does the orientation axis *z* lie in the threefold symmetry axis ($K_z > {}^1/_3 > K_y = K_x$) or perpendicular to it ($K_z = K_y > {}^1/_3 > K_x$)? If the former were true, $\sum_u K_u = K_z + 2K_y = 0.924$, and this differs from unity by far more than the experimental error. If the latter were true, $\sum_u K_u = 2K_z + K_x = 0.999$, and this equals unity within experimental error. Therefore, the threefold symmetry axis must lie perpendicular to the orientation axis, e vibrations must have the larger K value and positive dichroism, and a_1 vibrations must have the smaller K value and negative dichroism. These conclusions agree with the well-known assignments of the vibrational peaks of $CHCl_3$.

If all three K_u's are different, the assignment of the *x*, *y*, and *z* labels to individual molecular symmetry axes was based on (i) previous absolute IR polarization measurements (single crystals), or (ii) previous knowledge of K_u's from UV–visible polarization measurements, or (iii) the previous knowledge of the symmetry assignment and thus the polarization properties of specific IR transitions (C–halogen stretch, C–H out-of-plane bend of an olefin, etc.). This permitted absolute assignments in all but a few of the molecules.

A plot of K_z against K_y in the orientation triangle[4,5,21] (Figure 1) shows a clear relation between molecular shape and the orientation factors similar to that established earlier by UV–visible measurements for aromatic molecules:[5] the molecules tend to turn their smallest cross section in the direction of stretching. This result was then used to make absolute polarization assignments in the remaining molecules from their shapes.

Table II lists the detailed results for three selected triatomic molecules (Figure 2). In these cases the vibrational assignments have been well known for a long time, but the table provides a

(21) Michl, J.; Thulstrup, E. W. *Spectrosc. Lett.* **1977**, *10*, 401.
(22) In order to make the comparison more reliable, these spectra were measured on a single PE sample containing a mixture of the labeled and the unlabeled compound.

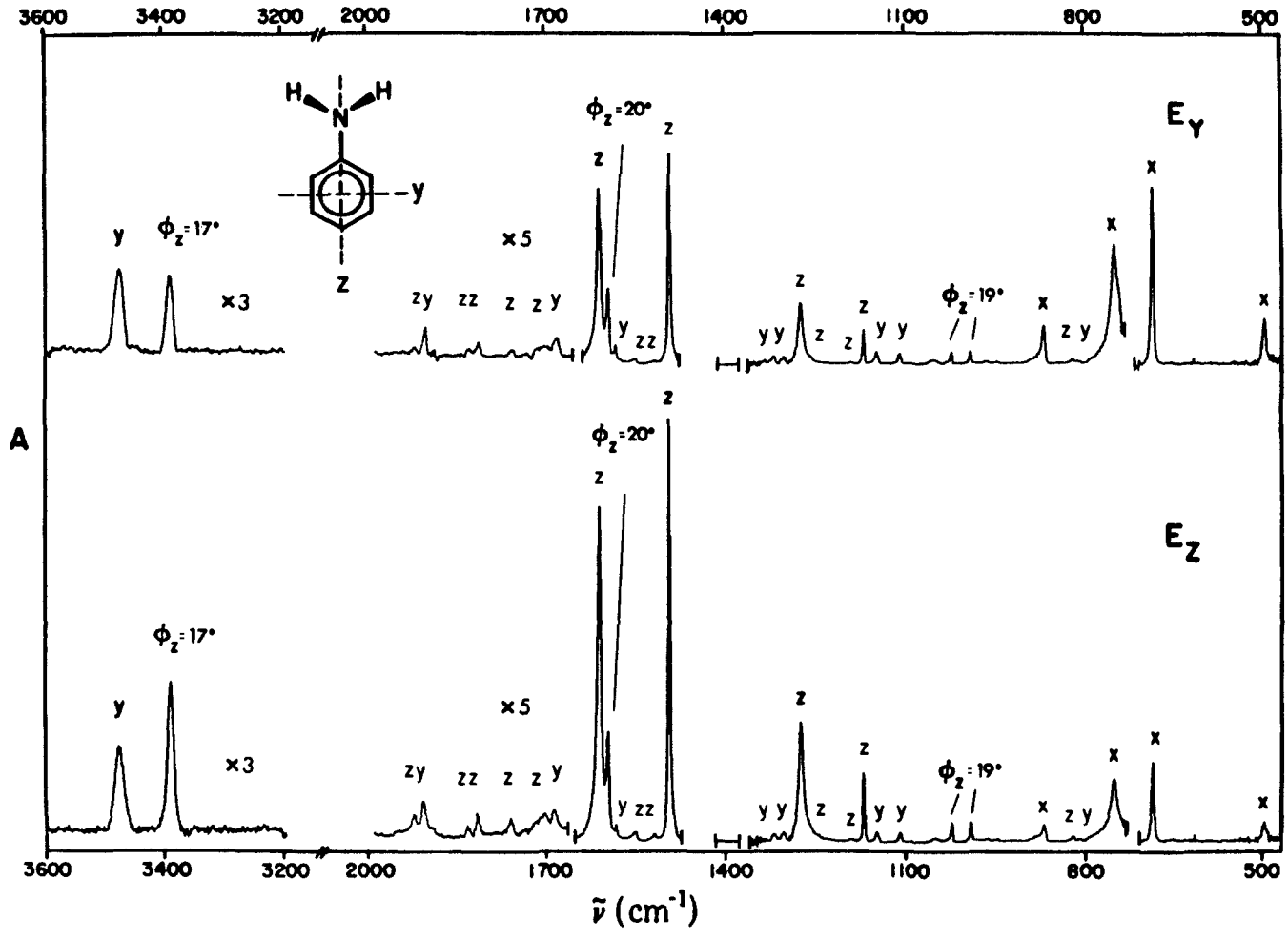

Figure 5. Polarized Fourier-transform IR spectra of aniline in stretched linear low-density polyethylene (12 K). In E_Z (E_Y), the electric vector of the light is oriented parallel (perpendicular) to the stretching direction Z. See also Table V and text.

feeling for the variation of the measured orientation factors from one observed band to another.

We do not list the observed vibrations and their symmetries for all of the molecules listed in Tables I and III since they can be readily measured whenever needed. Results for a few cases of special interest to us will be described in detail elsewhere (cf. ref 18).

For a limited number of compounds dichroic spectra were also measured at 77 K (Table III; Figure 3). In all cases lowering the temperature decreases the K_x value and increases K_z. For instance, for fluoranthene K_x(RT) = 0.11, K_x(77 K) = 0.07, and K_z(RT) = 0.58, K_z(77 K) = 0.61; for pyrene K_x(RT) = 0.12, K_x(77 K) = 0.10, and K_z(RT) = 0.52, K_z(77 K) = 0.56. The K_y value seems to be the least sensitive to temperature changes.

The isotopic effect of D vs. H on the orientation is very small, but detectable. It is presumably due to the effect of deuteration on effective molecular size and shape, related to anharmonicity and amplitude differences in the zero-point vibrational motion between H and D.

For the small molecules examined, the replacement of H with D in the solute leads to an increase in K_x and a decrease in K_y and K_z. For instance, at 77 K, we find for benzene, K_x = 0.24, $K_y = K_z$ = 0.37, and for benzene-d_6, K_x = 0.26, $K_y = K_z$ = 0.36; for chloroform K_x = 0.25, $K_y = K_z$ = 0.38 and for chloroform-d, K_x = 0.26, $K_y = K_z$ = 0.37. In the larger molecules, biphenyl and 4,4-dibromobiphenyl, the effect of deuteration is barely detectable at room temperature, although it is still quite distinct at low temperature.

IR Linear Dichroism and Molecular Geometry. We shall now describe our results for aniline in more detail and contrast them with those for nitrobenzene[23] in order to illustrate the application of IR linear dichroism to structural problems.

The application can take place at two levels. In the first place, it is possible to determine the number of different orientation factors K_f observed for the solute, and thus limit the point symmetry groups to which the solute molecule can possibly belong. At a more sophisticated level, it may be possible to determine valence and dihedral angles in the molecule. This requires a knowledge of the location of the molecular orientation axes, the measurement of the angles which IR transition moments form with the orientation axes, and the knowledge of the relation between the orientation of the IR transition moments of each vibration relative to the equilibrium positions of the atoms involved (e.g., the transition moment of a localized bond stretching vibration is oriented approximately along the bond).

The results for nitrobenzene and aniline are collected in Tables IV and V, respectively. The vibrations of nitrobenzene exhibit only three different K_f values within the experimental error, as expected for a molecule of D_{2h} symmetry. In particular, it is obvious that the nitro group is coplanar with the ring since the orientation factor of the antisymmetric combination of N–O stretching vibrations, 0.33, is equal to those of the other short in-plane axis-polarized vibrations (K_y).

In contrast, both in room temperature (RT) and in low-temperature (LT) measurements, the vibrations of aniline exhibit four different K_f values, proving that on the IR time scale the symmetry cannot be as high as D_{2h} or C_{2v}. The immediate suspicion is that the amino group is pyramidal in the solid solution similarly as it is known[24] to be in the gas phase, so that the symmetry is C_s.

(23) The IR linear dichroism of nitrobenzene in polyethylene and perdeuterated polyethylene has been described and used for symmetry assignments in an independent recent study by others.[16] Our results are in agreement.

Closer inspection of Table V confirms this conclusion. The orientation factor of the short in-plane axis is determined by the dichroism of the *as* NH_2 stretching vibration, and other vibrations of this polarization, for all of which $K_y^{RT} = 0.36$ ($K_y^{LT} = 0.33$). Several out-of-plane polarized vibrations have the orientation factor $K_x^{RT} = 0.20$ ($K_x^{LT} = 0.18$). The orientation factor of the long axis should therefore be $K_z^{RT} = 0.44$ ($K_z^{LT} = 0.49$), and these values are indeed observed for the C–N stretching vibration and a few others. These orientation factors are close to those of nitrobenzene.

However, the orientation factors of four other vibrations differ from the above three values by more than a possible experimental error (which is less than 0.01). In particular, the orientation factors of the symmetric NH_2 stretch ($K_\phi^{RT} = 0.41$, $K_\phi^{LT} = 0.47$) and of the NH_2 scissoring vibration (0.42 and 0.46, respectively) deviate from the value which would be expected if the NH_2 group were coplanar with the ring ($K_z^{RT} = 0.44$, $K_z^{LT} = 0.49$).

If it is assumed that effective molecular shape is C_{2v} due to relatively rapid pyramidal inversion of the NH_2 group (cf. the umbrella motion in NH_3), the principal orientation axes are dictated by the locations of the heavy atoms, with the z axis along the C–N bond and the x axis perpendicular to the aromatic ring. Such shape averaging would be slow on the IR time scale, so that IR transition moment directions would reflect the lower instantaneous symmetry C_s. It is then possible to use an expression valid for molecules of C_s symmetry[5]

$$\tan^2 \phi = (K_z - K_f)/(K_f - K_x) \qquad (4)$$

for the angle ϕ between the z axis and the moment direction of a transition f characterized by the orientation factor K_f and polarized in the xz plane. This yields $\phi = 21 \pm 5°$ (RT) and $\phi = 17 \pm 5°$ (LT) for the NH_2 symmetric stretch at 3393 cm^{-1} and $\phi = 17 \pm 5°$ (RT) and $\phi = 20 \pm 5°$ (LT) for NH_2 scissoring at 1602 cm^{-1}. If one assumes in the first approximation that these transitions are polarized along the bisectrix of the HNH angle, these results lead to $19 \pm 7°$ for the angle between the plane of the amino group and the plane of the ring. Also the polarization directions of the 995- and 1028-cm^{-1} vibrations lie at 19° to the z axis.

The angle between the HNH bisectrix and the z axis derived from IR dichroism in polyethylene is lower than the gas-phase microwave value,[24] 38°. Some of the discrepancy may be due to the effects of the polyethylene environment, but most of it is probably due to experimental inaccuracies and particularly to a deviation of the IR polarization directions from the bisectrix of the HNH angle.

Conclusion

We have demonstrated that Fourier-transform IR linear dichroism of high-symmetry nonpolar solutes in stretched polyethylene is readily measured and interpreted. We have not found a molecule which does not orient measurably unless demanded by symmetry (e.g., CCl_4). Even molecules as nearly spherical as the haloforms orient sufficiently for a reliable analysis. Finally, we have demonstrated on the simple examples of nitrobenzene and aniline how these measurements can be used for the determination of molecular symmetry.

The significance of this development is fourfold. First, it should greatly facilitate the analysis of and symmetry assignments in the vibrational spectra of complex molecules of high symmetry.[14-18] Second, it should be helpful in the structure and conformational analysis of those low-symmetry molecules which have characteristic vibrations with a priori known polarization directions. Third, it permits an unequivocal determination of orientation factors for studies of UV–visible dichroism and electronic transition moment direction.[25] Fourth, it permits a rapid acquisition of accurate values of the orientation factors for molecules of a variety of structures in a given stretched polymer, thus providing a basis for a future understanding of the detailed nature of the solute–polymer orienting interaction which is the object of much interest and speculation at present.[15,26] In this respect, it is superior to measurements of UV–visible dichroism: it is applicable to a larger number of molecular structures, it permits the independent measurement of all three K_u values, and it provides better statistics in that it usually offers a much larger number of transitions for any one solute.

The time now appears right to direct further work on structural applications to low-symmetry molecules. The theory for the evaluation of their linear dichroism is straightforward (e.g., ref 3 and 5), but the generally larger number of unknowns requires an increased amount of labor for each molecule. On the other hand, many of the most interesting conformational problems involve molecules with low or no symmetry.

Acknowledgment. This work was supported by the U.S. Army Research Office (DAAG 29-82-K-0024). The purchase of the FT-IR spectrometer was funded by the National Science Foundation (CHE-79-08823).

(24) Lister, D. G.; Tyler, J. K. *Chem. Commun.* **1966**, 152. For further references and discussion see: Niu, Z.; Boggs, J. E. *J. Mol. Struct. (Theochem.)* **1984**, *109*, 381.

(25) For examples see ref 10 and the following: Plummer, B. F.; Michl, J. *J. Org. Chem.* **1982**, *47*, 1233. Matsuoka, Y.; Nordén, B. *J. Phys. Chem.* **1982**, *86*, 1378; **1983**, *87*, 220.

(26) Konwerska-Hrabowska, J.; Kryszewski, M. *Bull. Acad. Pol. Sci., Ser. Sci. Math., Astron. Phys.* **1973**, *21*, 673, 771. Lamotte, M. *J. Chim. Phys.* **1975**, *72*, 803. Margulies, L.; Yogev, A. *Chem. Phys.* **1978**, *27*, 89. Dekkers, J. J.; Hoornweg, G. Ph.; Terpstra, K. J.; MacLean, C.; Velthorst, N. H. *Chem. Phys.* **1978**, *34*, 253. Bott, C. C.; Kurucsev, T. *Chem. Phys. Lett.* **1978**, *55*, 585. Jang, Y. T.; Phillips, P. J.; Thulstrup, E. W. *Chem. Phys. Lett.* **1982**, *93*, 66. Langkilde, F. W.; Gisin, M.; Thulstrup, E. W.; Michl, J. *J. Phys. Chem.* **1983**, *87*, 2901.

(27) Murthy, P. S.; Michl, J., manuscript in preparation.

(28) Kuwae, A.; Machida, K. *Spectrochim. Acta* **1979**, *35*, 27.

(29) Rai, J. N.; Maheshwari, R. C. *Current Sci. (India)* **1970**, *39*, 435. Evans, J. C. *Spectrochim. Acta* **1960**, *16*, 428.